

Large Matter Effects in $\nu_\mu \rightarrow \nu_\tau$ Oscillations

Raj Gandhi,¹ Pomita Ghoshal,¹ Srubabati Goswami,¹ Poonam Mehta,^{2,1} and S Uma Sankar³

¹ *Harish-Chandra Research Institute, Chhatnag Road, Jhansi, Allahabad 211 019, India*

² *Department of Physics and Astrophysics, University of Delhi, Delhi 110 019, India*

³ *Department of Physics, I. I. T., Powai, Mumbai 400 076, India*

(Dated: February 2, 2008)

We show that matter effects change the $\nu_\mu \rightarrow \nu_\tau$ oscillation probability by as much as 70% for certain ranges of energies and pathlengths. Consequently, the $\nu_\mu \rightarrow \nu_\mu$ survival probability also undergoes large changes. A proper understanding of ν_μ survival rates must consider matter effects in $P_{\mu\tau}$ as well as $P_{\mu e}$. We comment on a) how these matter effects may be observed and the sign of Δ_{31} determined in atmospheric neutrino measurements and at neutrino factories and b) how they lead to heightened sensitivity for small θ_{13} .

PACS numbers: 14.60.Pq, 14.60.Lm, 13.15.+g

Two of the most outstanding problems in neutrino physics are the determination of the mixing angle θ_{13} [1] and the sign of the atmospheric neutrino mass-difference Δ_{31} [2]. A knowledge of these parameters is crucial for understanding the form of the neutrino mass matrix. So far, most studies have concentrated on the $\nu_\mu \rightarrow \nu_e$ oscillation probability $P_{\mu e}$ as the means of determining the above parameters [6]. This is because the passage of neutrinos through earth matter dramatically changes $P_{\mu e}$.

In this letter we point out that the $\nu_\mu \rightarrow \nu_\tau$ oscillation probability $P_{\mu\tau}$ can also undergo significant change (a reduction as high as $\sim 70\%$ or an increase of $\sim 15\%$) compared to its vacuum values over an observably broad band in energies and baselines due to matter effects. This can also induce appreciable changes in the the muon neutrino survival probability $P_{\mu\mu}$ in matter.

The muon survival rate is the primary observable in iron calorimeter detectors like MINOS [7] and the proposed MONOLITH [8] and INO [9] and a major constituent of the signal in SuperKamiokande (SK) [5], the planned BNL-HomeStake [10] large water Cerenkov detector, and several detectors considered for future long baseline facilities. The τ appearance rate as a signal for matter effects can also be searched for in special τ detectors being thought of for neutrino factories [11]. We show that the energy ranges and baselines over which these effects occur are relevant for both atmospheric [12] and beam source neutrinos for the above experiments. Since all matter effects sensitively depend on the sign of Δ_{31} and on θ_{13} , observation of the effects discussed here would provide information on these important unknowns.

Our discussion below uses the approximation of constant density and sets $\Delta_{21} \equiv \Delta_{\text{sol}} = 0$. Consequently the mixing angle θ_{12} and the CP phase δ drop out of the oscillation probabilities. This simplifies the analytical expressions and facilitates the qualitative discussion of matter effects. We have checked that this works well (upto a few percent) at the energies and length scales relevant here. However, all the plots presented in this letter are obtained by numerically solving the full three flavour neutrino propagation equation assuming the PREM [13] density profile for the earth. Further, these

numerical calculations assume $\Delta_{21} = 8.2 \times 10^{-5} \text{ eV}^2$, $\sin^2 \theta_{12} = 0.27$ [14] and $\delta = 0$ [15]. We consider matter effects in neutrino probabilities only but discuss both the cases $\Delta_{31} = \pm |\Delta_{31}|$. We find that dramatic matter effects occur only for $\Delta_{31} > 0$.

Review of $P_{\mu e}$ in matter: In vacuum, the $\nu_\mu \rightarrow \nu_e$ oscillation probability is

$$P_{\mu e}^{\text{vac}} = \sin^2 \theta_{23} \sin^2 2\theta_{13} \sin^2 (1.27 \Delta_{31} L/E), \quad (1)$$

where $\Delta_{31} \equiv m_3^2 - m_1^2$ is expressed in eV^2 , L in Km and E in GeV. In the constant density approximation, matter effects can be taken into account by replacing Δ_{31} and θ_{13} in Eq. (1) by their matter dependent values,

$$\begin{aligned} \Delta_{31}^{\text{m}} &= \sqrt{(\Delta_{31} \cos 2\theta_{13} - A)^2 + (\Delta_{31} \sin 2\theta_{13})^2} \\ \sin 2\theta_{13}^{\text{m}} &= \sin 2\theta_{13} \Delta_{31} / \Delta_{31}^{\text{m}} \end{aligned} \quad (2)$$

where $A = 2\sqrt{2}G_F n_e E$ is the Wolfenstein term. The resonance condition is $A = \Delta_{31} \cos 2\theta_{13}$, which gives $E_{\text{res}} = \Delta_{31} \cos 2\theta_{13} / 2\sqrt{2}G_F n_e$. Naively, one would expect $P_{\mu e}^{\text{mat}}$ to be maximum at $E = E_{\text{res}}$ since $\sin 2\theta_{13}^{\text{m}} = 1$. But this is not true in general because at this energy Δ_{31}^{m} takes its minimum value of $\Delta_{31} \sin 2\theta_{13}$ and $P_{\mu e}^{\text{mat}}$ remains small for pathlengths of $L \leq 1000$ Km. $P_{\mu e}^{\text{mat}}$ is maximum when both $\sin 2\theta_{13}^{\text{m}} = 1$ and $\sin^2 (1.27 \Delta_{31}^{\text{m}} L/E) = 1 = \sin^2 [(2p+1)\pi/2]$ are satisfied. This occurs when $E_{\text{res}} = E_{\text{peak}}^{\text{mat}}$. This gives the condition [16]:

$$\rho L_{\mu e}^{\text{max}} \simeq \frac{(2p+1)\pi 5.18 \times 10^3}{\tan 2\theta_{13}} \text{ Km gm/cc.} \quad (3)$$

Here, p takes integer values. This condition is independent of Δ_{31} but depends sensitively on θ_{13} . Using the product $\rho_{\text{av}} L$ vs L for the earth (calculated using the PREM profile), where ρ_{av} is the average density for a given baseline L , we identify the particular values of $\rho_{\text{av}} L$ which satisfy Eq. (3) with $p=0$ for three different values of $\sin^2 2\theta_{13}$. These occur at $L \simeq 10200$ Km, 7600 Km and 11200 Km for $\sin^2 2\theta_{13} = 0.1, 0.2$ and 0.05 respectively. Note that $p=0$ is the only relevant value of p in this case,

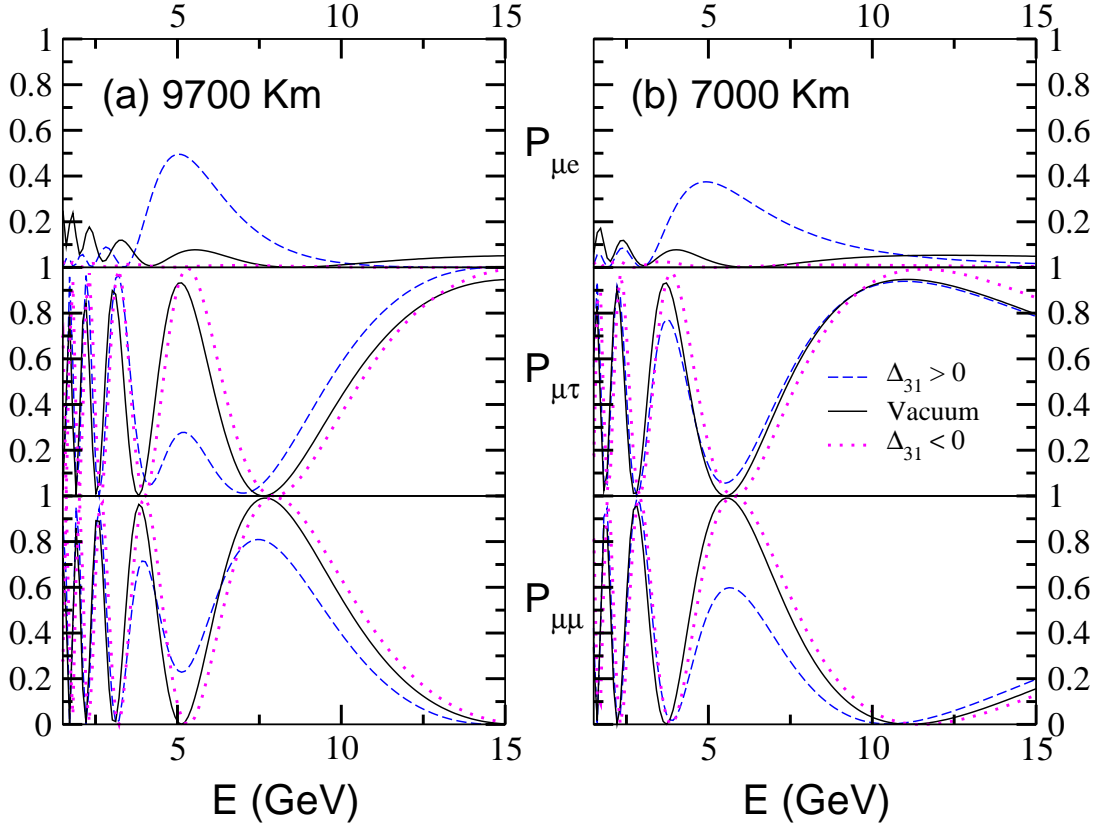


FIG. 1: $P_{\mu e}$, $P_{\mu \tau}$ and $P_{\mu \mu}$ plotted versus neutrino energy, E (in GeV) in matter and in vacuum for both signs of Δm_{31}^2 for two different baseline lengths, (a) for $L=9700$ Km and (b) for $L=7000$ Km. These plots use $\Delta_{31} = 0.002 \text{ eV}^2$ and $\sin^2 2\theta_{13} = 0.1$.

given earth densities and baselines [17].

Matter effects in $P_{\mu \tau}$: In vacuum we have

$$\begin{aligned} P_{\mu \tau}^{\text{vac}} &= \cos^4 \theta_{13} \sin^2 2\theta_{23} \sin^2 (1.27 \Delta_{31} L/E), \\ &= \cos^2 \theta_{13} \sin^2 2\theta_{23} \sin^2 (1.27 \Delta_{31} L/E) \\ &\quad - \cos^2 \theta_{23} P_{\mu e}^{\text{vac}} \end{aligned} \quad (4)$$

Including the matter effects [18] changes this to

$$\begin{aligned} P_{\mu \tau}^{\text{mat}} &= \cos^2 \theta_{13}^{\text{m}} \sin^2 2\theta_{23} \sin^2 [1.27(\Delta_{31} + A + \Delta_{31}^{\text{m}})L/2E] \\ &\quad + \sin^2 \theta_{13}^{\text{m}} \sin^2 2\theta_{23} \sin^2 [1.27(\Delta_{31} + A - \Delta_{31}^{\text{m}})L/2E] \\ &\quad - \cos^2 \theta_{23} P_{\mu e}^{\text{mat}} \end{aligned} \quad (5)$$

Compared to $P_{\mu e}^{\text{mat}}$, the matter dependent mass eigenstates here have a more complicated dependance on the ν_{μ} and ν_{τ} flavour content. Labeling the vacuum mass eigenstates as ν_1 , ν_2 and ν_3 , ν_1 can be chosen to be almost entirely ν_e and ν_2 to have no ν_e component [19]. Inclusion of the matter term A leaves ν_2 untouched but gives a non-zero matter dependent mass to ν_1 . As the energy increases, the ν_e component of ν_1^{m} decreases and the ν_{μ}, ν_{τ} components increase such that at resonance energy they are 50%. Similarly, increasing energy increases the ν_e component of ν_3^{m} (and reduces ν_{μ}, ν_{τ} components) so that at resonance it becomes 50%. Thus in

the resonance region, all three matter dependent mass eigenstates $\nu_1^{\text{m}}, \nu_2^{\text{m}}$ and ν_3^{m} contain significant ν_{μ} and ν_{τ} components.

We seek ranges of energy and pathlengths for which there are large matter effects in $P_{\mu \tau}$, i.e for which $\Delta P_{\mu \tau} = P_{\mu \tau}^{\text{mat}} - P_{\mu \tau}^{\text{vac}}$ is large. We show that this occurs for two different sets of conditions, leading in one case to a decrease from a vacuum maximum and in another to an increase over a broad range of energies.

(i) **Large decrease in $P_{\mu \tau}^{\text{mat}}$ in the resonance region:** At energies appreciably below resonance, the $\cos^2 \theta_{13}^{\text{m}}$ term in Eq. (5) $\approx P_{\mu \tau}^{\text{vac}}$ (since $\theta_{13}^{\text{m}} = \theta_{13}$, $A \ll \Delta_{31}, \Delta_{31}^{\text{m}} \approx \Delta_{31}$) and the $\sin^2 \theta_{13}^{\text{m}}$ term is nearly zero. As we increase the energy and approach resonance, $\cos^2 \theta_{13}^{\text{m}}$ begins to decrease sharply, while $\sin^2 \theta_{13}^{\text{m}}$ increases rapidly. However, if resonance is in the vicinity of a vacuum peak, then the decrease in the $\cos^2 \theta_{13}^{\text{m}}$ term has a much stronger impact on $P_{\mu \tau}^{\text{mat}}$ than the increase in the $\sin^2 \theta_{13}^{\text{m}}$ term, since the latter starts out at zero while the former is initially close to its peak value (≈ 1). As a result, $P_{\mu \tau}^{\text{mat}}$ falls sharply. This fall is enhanced by the third term in Eq. (5), which is essentially $0.5 \times P_{\mu e}^{\text{mat}}$ (which is large due to resonance), leading to a large overall drop in $P_{\mu \tau}^{\text{mat}}$ from its vacuum value. Note that the requirement that we be at a vacuum peak to begin with forces $\Delta P_{\mu \tau}$ to be large and negative, with the contribu-

tions from the first and the third term reinforcing each other.

The criterion for maximal matter effect, $E_{\text{res}} \simeq E_{\text{peak}}^{\text{vac}}$, leads to the following condition:

$$\rho L_{\mu\tau}^{\text{max}} \simeq (2p+1) \pi 5.18 \times 10^3 (\cos 2\theta_{13}) \text{ Km gm/cc.} \quad (6)$$

Unlike Eq. (3), which has a $\tan 2\theta_{13}$ in its denominator, Eq. (6) has a much weaker dependence on θ_{13} . This enables one to go to a higher value of p without exceeding the baselines relevant for observing earth matter effects. Incorporating the $E_{\text{res}} = E_{\text{peak}}^{\text{vac}}$ condition we get $\Delta P_{\mu\tau}$ as

$$\Delta P_{\mu\tau} \simeq \cos^4 \left[\sin 2\theta_{13} (2p+1) \frac{\pi}{4} \right] - 1 \quad (7)$$

where we approximated $\cos 2\theta_{13} \simeq 1$. We note that, in general, $\Delta P_{\mu\tau}$ will be larger for higher values of both p and θ_{13} . From Eq. (6), for $p=1$ and $\sin^2 2\theta_{13} = 0.1(0.2, 0.05)$, $E_{\text{res}} = E_{\text{peak}}^{\text{vac}}$ occurs at ~ 9700 Km (9300 Km, 9900 Km) and $\Delta P_{\mu\tau} \approx -0.7$ (from Eq. (7)). For $p=0$, Eq. (6) gives $L_{\mu\tau}^{\text{max}} \sim 4400$ Km for $\sin^2 2\theta_{13} = 0.1$. However, $\Delta P_{\mu\tau}$ is roughly one-tenth of the $p=1$ case. In general, for a given baseline, the choice of an optimal p is also dictated by the constraint that the vacuum peak near resonance have a breadth which makes the effect observationally viable.

In Fig. 1(a) we show all three matter and vacuum probabilities for 9700 Km. In these plots Δ_{31} is taken as 0.002 eV^2 , which gives $E_{\text{res}} = E_{\text{peak}}^{\text{vac}} \sim 5 \text{ GeV}$. The middle panel of Fig. 1(a) shows that near this energy $P_{\mu\tau}^{\text{mat}}$ (~ 0.33) is appreciably lower compared to $P_{\mu\tau}^{\text{vac}}$ (~ 1). Thus the drop due to matter effect is 0.67, which agrees well with that obtained earlier using the approximate expression Eq. (7).

In Fig. 2 we show the θ_{13} sensitivity of $P_{\mu\tau}^{\text{mat}}$ at 9700 Km. In particular, at $E_{\text{res}} \simeq E_{\text{peak}}^{\text{vac}}$ the strong dependence on θ_{13} is governed by Eq. (7) above. Unlike $P_{\mu\tau}^{\text{mat}}$, where the event-rate decreases as θ_{13}^2 for small values of θ_{13} , the τ appearance rate at $E_{\text{res}} = E_{\text{peak}}^{\text{vac}}$ increases with decreasing θ_{13} . As $\sin^2 2\theta_{13}$ goes from 0.2 to 0, $P_{\mu\tau}^{\text{mat}}$ varies from ~ 0.05 to ~ 1 . For very small values of $\sin^2 2\theta_{13} (< 0.05)$ it will be impossible to see a *maximal* resonance enhancement in $P_{\mu\tau}$ because the distance for which this occurs exceeds the diameter of the earth. However, the observation of resonant suppression in $P_{\mu\tau}$ is possible, even for very small values of θ_{13} , if the criterion, $N_{\tau}(\theta_{13} = 0) - N_{\tau}(\theta_{13}) \geq 3(\sqrt{N_{\tau}(\theta_{13} = 0)} + \sqrt{N_{\tau}(\theta_{13})})$, is satisfied for the tau event rate.

In general the resonance has a width, and this fact affects observability. To include the width of the resonance, we write $A = \Delta_{31}(\cos 2\theta_{13} + q \sin 2\theta_{13})$. We find that the large matter effects discussed above still do occur as long as A is within the width of the resonance or $-1 \leq q \leq 1$.

(ii) **Increase in $P_{\mu\tau}$ away from resonance :** It is also possible for $P_{\mu\tau}^{\text{mat}}$ to differ appreciably from $P_{\mu\tau}^{\text{vac}}$ away from resonance. This is evident in Fig. 1(a) (central panel) in the energy range 7.5 GeV - 15 GeV. This

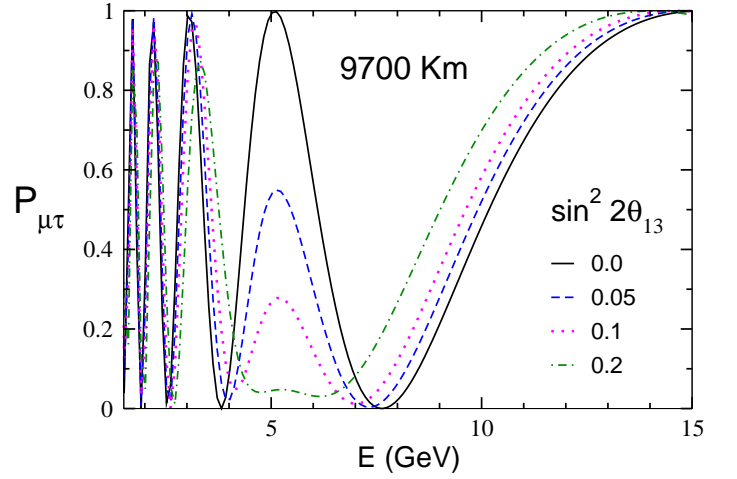


FIG. 2: $P_{\mu\tau}$ plotted against the neutrino energy, E (in GeV) for different values of θ_{13} . We have used $\Delta_{31} = 0.002 \text{ eV}^2$.

effect is an enhancement rather than a drop, *i.e.*, $\Delta P_{\mu\tau}$ is now positive. $\Delta P_{\mu\tau}$ is small in most of the latter part of the energy region under consideration and does not contribute in an important way overall. The dominant contribution to this enhancement arises from the $\sin^2 \theta_{13}^m$ term in $P_{\mu\tau}$ (Eq. (5)) which is large for $E \gg E_{\text{res}}$. Since $(\Delta_{31} + A - \Delta_{31}^m) \approx 2 \Delta_{31}$ for these energies, we obtain an enhancement ($\sim 15\%$) which follows the vacuum curve. The difference between the vacuum and matter curves largely reflects the difference between the $\cos^4 \theta_{13}$ multiplicative term in the vacuum expression Eq. (4) and the $\sin^2 \theta_{13}^m$ multiplicative term in Eq. (5). While this effect is smaller compared to the effect in (i) above, it occurs over a broad energy band and may manifest itself in energy integrated event rates.

Finally, we comment on the observability of the matter effects in $P_{\mu\tau}$. The energies in question are above, but close to the τ production threshold. This suppresses the τ appearance rates, and will necessitate a high luminosity beam experiment. Such direct observation must perhaps await the advent of superbeams and/or neutrino factories. However, the effects in $P_{\mu\tau}^{\text{mat}}$ manifest themselves indirectly in $P_{\mu\mu}^{\text{mat}}$, as we discuss below, and these can be observed in an atmospheric neutrino experiment.

Matter effects in $P_{\mu\mu}$: The deviation of $P_{\mu\mu}^{\text{mat}}$ from $P_{\mu\mu}^{\text{vac}}$ clearly results from the combined effects in $P_{\mu\tau}^{\text{mat}}$ and $P_{\mu\mu}^{\text{vac}}$ *i.e.* $\Delta P_{\mu\mu} = -\Delta P_{\mu\tau} - \Delta P_{\mu\mu}$.

In case (i) above, for instance, $\Delta P_{\mu\tau}$ is large and negative while $\Delta P_{\mu\mu}$ is positive and hence they do not contribute in consonance. However, the resulting change in $P_{\mu\mu}$ is still large, given the magnitude of the change ($\approx 70\%$) in $P_{\mu\tau}$. This is visible in the bottom panel of Fig. 1(a), in the energy range 4-6 GeV.

One also expects a significant drop in $P_{\mu\mu}^{\text{mat}}$ when either of $\Delta P_{\mu\tau}$ or $\Delta P_{\mu\mu}$ is large and the other one is small. The first of these cases ($\Delta P_{\mu\tau}$ large, $\Delta P_{\mu\mu}$ small) is shown in Fig. 1(a) in the energy range $\sim 6 - 15 \text{ GeV}$, with the

enhancement in $P_{\mu\tau}^{\text{mat}}$ reflected in the decrease in $P_{\mu\mu}^{\text{mat}}$. The second case (small $\Delta P_{\mu\tau}$, large $\Delta P_{\mu e}$) occurs when a minimum in the vacuum value of $P_{\mu\tau}$ resides in the proximity of a resonance, and even the rapid changes in $\sin^2 \theta_{13}^m$ and $\cos^2 \theta_{13}^m$ in this region fail to modify this small value significantly. This condition can be expressed as $1.27\Delta_{31}L/E = p\pi$. Note that this corresponds to a vacuum peak of $P_{\mu\mu}$. Substituting E as E_{res} gives the distance for maximum matter effect in $P_{\mu\mu}$ as

$$\rho L_{\mu\mu}^{\text{max}} \simeq p\pi \times 10^4 (\cos 2\theta_{13}) \text{ Km gm/cc} \quad (8)$$

For $p=1$ this turns out to be ~ 7000 Km. This effect [21] is shown in the bottom panel of Fig. 1(b). The large (40% at its peak) drop in $P_{\mu\mu}$ seen in this figure derives its strength from the resonant enhancement in $P_{\mu e}$. A sensitivity to θ_{13} around the peak similar to the one discussed above for $P_{\mu\tau}^{\text{mat}}$ also exists here, leading to a larger muon survival rate as θ_{13} becomes smaller.

The width of both these effects is significant, ranging from 4 – 10 GeV in the first case (Fig. 1(b)) and 6 – 15 GeV in the second. We have checked that they persist over a range of baselines (6000 - 9700 Km), making them observationally feasible.

Observational Possibilities and Conclusions: We have shown that large matter effects in neutrino oscillations are not necessarily confined to $\nu_\mu \rightarrow \nu_e$ or $\nu_e \rightarrow \nu_\tau$ conversions, but can be searched for in $\nu_\mu \rightarrow \nu_\tau$ oscillation and $\nu_\mu \rightarrow \nu_\mu$ survival probabilities. We have discussed their origin by studying the inter-relations of all the three matter probabilities, $P_{\mu e}^{\text{mat}}$, $P_{\mu\tau}^{\text{mat}}$ and $P_{\mu\mu}^{\text{mat}}$, and identified baseline and energy ranges where they act co-

herently to give observationally large effects. The effects discussed are strongly sensitive to the sign of Δm_{31}^2 , as is apparent in the figures above. Also, there is sensitivity to small θ_{13} at the energy and baseline ranges identified for $P_{\mu\tau}^{\text{mat}}$ and $P_{\mu\mu}^{\text{mat}}$.

Specialized τ detectors operating in long baseline scenarios [11] should be able to observe effects like the ones discussed in the central panel of Fig. 1(a) and in Fig. 2. Similarly, detectors capable of measuring muon survival rates, e.g. magnetized iron calorimeters can detect the effects visible in the bottom panels of Fig. 1(a) and (b) [20]. To illustrate the observability of the effect, we calculate that for a magnetized iron calorimeter detector [8, 9] and an exposure of 1000 kT-yr, in the energy range 5 - 10 GeV and Lrange of 6000 - 9700 Km, with $\Delta_{31} = +0.002 \text{ eV}^2$ and $\sin^2 2\theta_{13} = 0.1$, the total number of atmospheric μ^- events in the case of vacuum oscillations is 261. However, it reduces to 204 with matter effects. The rates for μ^+ in matter are identical to the vacuum value of 105 events. These numbers reflect a 4σ signal for the effect discussed above for $P_{\mu\mu}^{\text{mat}}$ [22]. The Fermilab to Kamioka proposal [23] has a baseline of 9300 Km and is within the range of baselines where these effects are large and observable.

Finally, we remark that although the effects discussed here appear only for ν_μ for Δ_{31} positive (and only for $\bar{\nu}_\mu$ for Δ_{31} negative) it may still be possible to search for them in the accumulated SK data.

Acknowledgments : PM acknowledges CSIR, India for partial financial support and HRI and INO for hospitality.

-
- [1] The current bound on θ_{13} is $\sin^2 \theta_{13} < 0.05$ (3σ) [3]. However, this is sensitive to the value of Δ_{31} [4].
 - [2] The best-fit value of Δ_{31} from zenith angle analysis of SK data is $2.1 \times 10^{-3} \text{ eV}^2$ [5].
 - [3] A. Bandyopadhyay *et al.* hep-ph/0406328.
 - [4] S. Goswami, talk at Neutrino 2004.
 - [5] E. Kearns, talk at Neutrino 2004.
 - [6] See e.g. I. Mocioiu and R. Shrock, Phys. Rev. D **62**, 053017 (2000); V. Barger *et al.*, *ibid.* **62**, 013004 (2000); *ibid.* Phys. Lett. B **485**, 379 (2000), hep-ph/0004208; E. K. Akhmedov *et al.*, JHEP **0404**, 078 (2004) and references therein.
 - [7] R. Saakian, Nucl. Phys. Proc. Suppl. **111**, 169 (2002).
 - [8] N. Y. Agafonova *et al.*, LNGS-P26-2000; <http://castore.mi.infn.it/~monolith/>
 - [9] See <http://www.imsc.res.in/~ino>.
 - [10] M. Diwan *et al.*, hep-ex/0211001.
 - [11] C. Albright *et al.*, hep-ex/0008064.
 - [12] Matter effects for atmospheric neutrinos are also discussed e.g. in E. K. Akhmedov *et al.* Nucl. Phys. B **542**, 3 (1999); J. Bernabeu *et al.*, Phys. Lett. B **531**, 90 (2002).
 - [13] We use the parametrization given in R. Gandhi *et al.*, Astropart. Phys. **5**, 81 (1996).
 - [14] T. Araki *et al.*, hep-ex/0406035.
 - [15] We checked that for $\delta = \pm\pi/2$ the change is within 10%.
 - [16] M. C. Banuls *et al.*, Phys. Lett. B **513**, 391 (2001).
 - [17] The approximation of “average constant density” is not a good one for core passage but is included here since it delineates the range of $\sin^2 2\theta_{13}$ where core passage is a requisite for maximal matter effects.
 - [18] See the third and fourth references in [6].
 - [19] While θ_{12} is undetermined in the approximation $\Delta_{21} = 0$, it also drops out of the mixing matrix in this approximation, and the weights of ν_e in ν_1 and ν_2 do not depend on it.
 - [20] T. Tabarelli de Fatis, Eur. Phys. J. C **24**, 43 (2002); S. Palomares-Ruiz and S. T. Petcov, hep-ph/0406096; D. Indumathi and M.V.N. Murthy, hep-ph/0407336.
 - [21] See the first reference in [6]. Also see [16] and the second reference in [20].
 - [22] R. Gandhi *et al.*, HRI Preprint, HRI-P-04-10-002.
 - [23] F. DeJongh, arXiv:hep-ex/0203005.